Materials Letters 105 (2013) 72–75

Contents lists available at SciVerse ScienceDirect

Materials Letters

journal homepage: www.elsevier.com/locate/matlet

Microstructural and optical properties of ZrON/Si thin films

V.V. Atuchin [a,*], V.N. Kruchinin [b], Yew Hoong Wong [c,d], Kuan Yew Cheong [e]

[a] Laboratory of Optical Materials and Structures, Institute of Semiconductor Physics, SB RAS, Novosibirsk 90, Novosibirsk 630090, Russia
[b] Laboratory for Ellipsometry of Semiconductor Materials and Structures, Institute of Semiconductor Physics, SB RAS, Novosibirsk 90, Novosibirsk 630090, Russia
[c] Department of Mechanical Engineering, Faculty of Engineering, University of Malaya, 50603 Kuala Lumpur, Malaysia
[d] Centre of Advanced Manufacturing and Material Processing, University of Malaya, 50603 Kuala Lumpur, Malaysia
[e] Electronic Materials Research Group, School of Materials and Mineral Resources Engineering, Engineering Campus, Universiti Sains Malaysia, 14300 Nibong Tebal, Penang, Malaysia

ARTICLE INFO

Article history:
Received 26 February 2013
Accepted 20 March 2013
Available online 30 March 2013

Keywords:
ZrON/Si structure
SEM
AFM
Spectroscopic ellipsometry

ABSTRACT

ZrON/Si(100) layer structure formation has been produced by oxidation/nitridation of sputtered Zr metal in N_2O/Ar ambient at 500–900 °C. Micromorphology and structural properties of the films have been evaluated by scanning electron microscopy, atomic force microscopy, and reflection high-energy electron diffraction. Dispersive optical properties of the ZrON/Si reflection system have been studied with spectroscopic ellipsometry. A drastic increase of SiO_2-based interface layer thickness has been found at 700–900 °C.

1. Introduction

The scaling of electronic devices based on such key semiconductor materials as Si, Ge, GaN, and SiC requires the reduction of gate dielectric thickness and a search for new dielectric materials with high permittivity and low leakage current [1–3]. Many high dielectric constant (k) oxides have been proposed and evaluated during recent years and ZrO_2-based compounds are considered among the most promising materials for the nearest future generation nodes [1–10]. Commonly, ZrO_2 is widely used in modern technology because of its excellent chemical stability, high mechanical and thermal properties, high refractive index, and wide optical transparency range [1,2,11–15]. Thin films of ZrO_2 oxide in amorphous and crystalline states can be deposited by different methods and microstructural and optical properties of the films are strongly dependent on real defect structure, including oxygen vacancies. Recently, the interesting technology of zirconium oxynitride formation by direct chemical oxidation/nitridation of Zr metal films in N_2O gas flow at high temperature has been developed [16–18]. The interface layer formation with an intermediate chemical composition was found in ZrON/Si and ZrON/4 · H-SiC systems by depth-profiling X-ray photoelectron spectroscopy (XPS) analysis. As it was shown, the interface layer in the ZrON/Si system contains the dominant part of nitrogen introduced by oxidation/nitridation process [16]. The present study is aimed at the complex evaluation of microstructural and optical properties of the ZrON/Si film system to reveal the parameters of the interface layer in detail. For this purpose, the high-quality ZrON/Si films were grown onto Si(100) substrates at different reaction temperatures.

2. Experimental

The n-type Si(100) substrates with resistivity 1–10 Ω cm were cleaned by a standard Radio Corporation of America (RCA) cleaning method and treated with a diluted HF solution (1 HF:50 · H_2O) for 15 s to remove the native oxide from the surface prior to Zr metal sputtering. Edwards Auto 500 radio frequency (RF) sputtering system was used to deposit an ultrathin 5-nm Zr metal thin film on the cleaned Si substrates using an Alfa Aesar Zr metal target with the purity of 99.5%. The RF power, working pressure, inert Ar gas flow and deposition rate were regulated to be at the level of 170 W, 1.2×10^{-7} Torr, 20 cm^3/min, and 0.2 nm/s, respectively. The oxidation/nitridation of Zr metal layer was performed after the deposition. The Zr/Si samples were placed into a horizontal tube furnace and heated up from room temperature to a set of temperatures (500, 700 and 900 °C) in an Ar flow ambient and the heating rate was constant at 10 °C/min. Once the set temperature was reached, N_2O gas was then purged in with a flow rate of 150 mL/min for 15 min to form the ZrON/Si layer. Then, the samples were eventually taken out at room temperature after the furnace had been cooled down to room temperature in an Ar ambient.

Thin film surface micromorphology was examined by a field-emission scanning electron microscope (FESEM) (Zeiss Supra 35VP).

* Corresponding author. Tel.: +7 383 3308889; fax: +7 383 3332771.
E-mail addresses: atuchin@isp.nsc.ru, atuchin@thermo.isp.nsc.ru (V.V. Atuchin).

0167-577X/$ - see front matter © 2013 Elsevier B.V. All rights reserved.
http://dx.doi.org/10.1016/j.matlet.2013.03.100

The surface topography and roughness of the ZrON/Si thin film surfaces were analyzed by an atomic force microscope (AFM) (NanoNavi SPI3800N) using a non-contact mode. The AFM was equipped with a Si_3N_4 cantilever, and the AFM topographies were recorded on a $1\times1\ \mu m^2$ scanned area. The top-surface crystallographic properties were evaluated with reflection high-energy electron diffraction (RHEED) using an EFZ4 device under electron energy 50 keV.

Dispersive refractive index $n(\lambda)$ and extinction coefficient $k(\lambda)$ were determined by means of spectroscopic ellipsometry (SE). Ellipsometric angles Ψ and Δ were measured as a function of λ in the spectral range of λ~250–1030 nm using an ELLIPS-1771 SA ellipsometer [19]. The instrumental spectral resolution was 2 nm, and the recording time of the spectrum did not exceed 20 s. The SE measurements were produced at three angles of incidence of light beam on the sample of 50°, 60° and 70°. The four-zone measurement method was used with subsequent averaging over all the four zones. Ellipsometric parameters Ψ and Δ are related to the complex Fresnel reflection coefficients by the equation

$$tg\psi\, e^{i\Delta} = \frac{R_p}{R_s} \tag{1}$$

where R_p and R_s are the coefficients for p- and s-polarized light-waves. To calculate the dependencies of refractive index $n(\lambda)$ and extinction coefficient $k(\lambda)$ on optical wavelength λ, the experimental data were processed using the two-layer model of (air)–(homogeneous isotropic ZrON layer)–(homogeneous isotropic interface layer)–(homogeneous isotropic Si substrate). The optical parameters of interface film were taken as related to SiO_2 oxide [20]. Thus, over the whole spectral range, the spectral dependences of polarization angles were fitted for m points of the spectrum by minimization of the error function

$$\sigma^2 = \frac{1}{m}\sum_{i=1}^{m}[(\Delta_{exp}-\Delta_{calc})^2 + (\psi_{exp}-\psi_{calc})^2] \tag{2}$$

Dispersion functions $n(\lambda)$ and $k(\lambda)$ were approximated by Cauchy's polynomials [21,22]:

$$n(\lambda) = a + \frac{b}{\lambda^2} + \frac{c}{\lambda^4}, k(\lambda) = d + \frac{e}{\lambda^2} + \frac{f}{\lambda^4} \tag{3}$$

where a, b, c, d, e and f are constants, which are specific to the material.

3. Results and discussion

A typical FESEM image of the ZrON/Si film is shown in Fig. 1. FESEM surface inspection using low (100×) to high (10k×) magnification did not reveal any observable defects, such as a crack or a void on all ZrON thin films grown at different temperatures. This indicates that the produced film is smooth and uniform. There is no noticeable variation of the top surface micromorphology on oxidation/nitridation temperature change and FESEM images recorded for the samples made at 500 and 900 °C are shown in Figs. 1S and 2S. The RMS surface roughness of all the investigated samples is shown in Fig. 2, and the inset demonstrates a typical three-dimensional surface topography of the sample oxidized/nitrided at 700 °C. Here, the scanned area is $1\times1\ \mu m^2$. The RMS surface roughness evidently increases from 0.49 to 1.12 nm as the reaction temperature increases from 500 °C to 900 °C. The increment of RMS roughness is related to activation of atom ordering and grain formation process at higher temperatures. Previously, initial stages of crystallization in the film bulk (ZrO_2) were detected by X-ray diffraction (XRD) analysis in the ZrON/Si film treated in N_2O at 700 °C for 5–20 min [16]. Nevertheless, the top-surface of the film remains to be amorphous for the temperature range of 500–900 °C as it is verified by RHEED

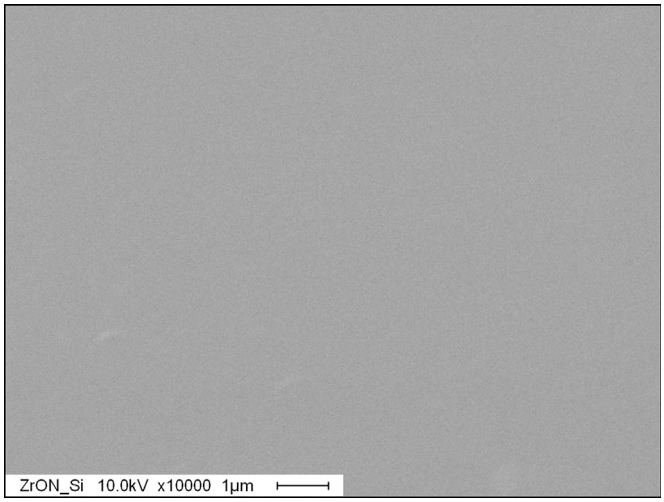

Fig. 1. Typical FESEM micrograph of a ZrON/Si film prepared at 700 °C.

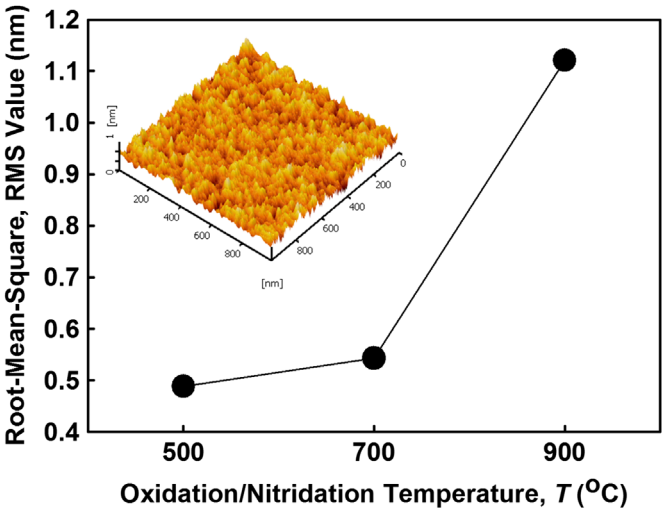

Fig. 2. The RMS value of investigated samples as a function of oxidation/nitridation temperature. The inset shows three-dimensional AFM topography of the sample treated at 700 °C.

observation in the present study. As an example, the RHEED patterns recorded from the Si(100) substrate and ZrON film are shown in Fig. 3S. Kikuchi-line pattern is evident for the initial Si substrate, and only amorphous halo is recorded from ZrON surface.

The ellipsometric parameters $\Psi(\lambda)$ and $\Delta(\lambda)$ measured at $\varphi=70°$ and calculated are shown in Fig. 4S for the samples treated at 500, 700 and 900 °C. The related curves obtained at $\varphi=50$ and 60° were also analyzed, but are not shown here to save space. The experimental results measured from the film formed at 500 °C can be well approximated by the model curves at the zero interface layer thickness. For the films formed at 700 and 900 °C, introduction of the interface layer between the ZrON layer and Si substrate is inevitably necessary to solve the inverse ellipsometric problem. It should be pointed out that formation of the interface layer at 700 °C dominated by silicon oxide was previously detected by XPS depth profiling [16]. The results of optical parameters simulation of the reflection layer systems using Cauchy's relations are shown in Table 1. It is evident that the interface layer thickness increases swiftly with the oxidation/nitridation temperature increase. Comparatively, the thickness of ZrON layer is nearly the same at all synthesis temperatures and is governed by the initial Zr metal thickness. At 500 °C, the oxidation of zirconium seems to be

Table 1
Thickness values and Cauchy parameters obtained from the ZrON/SiO_2/Si(100) layer systems prepared at different temperatures.

Synthesis temperature (°C)	Thickness SiO_2 (nm)	Thickness ZrON (nm)	Cauchy parameters of ZrON			
			a	$b \times 10^{-4}$	$c \times 10^{-9}$	σ
500	–	18.02	1.811	4.716	−1.904	5.5
700	6.8	23.06	1.948	−0.441	1.435	7.5
900	33.8	21.91	1,937	−0,167	1.108	13.7

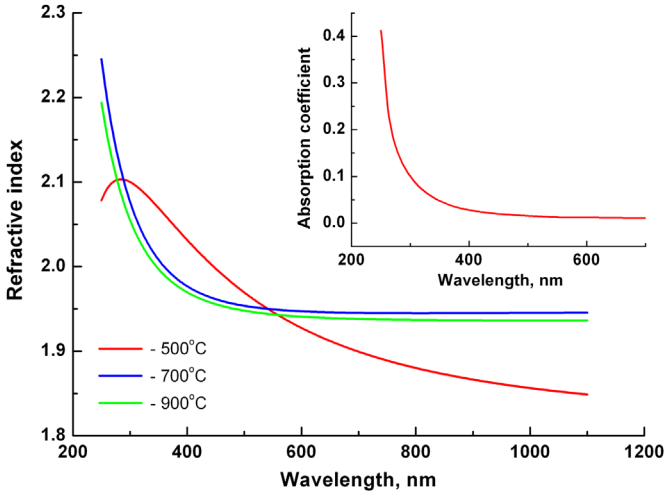

Fig. 3. Dispersive refractive index $n(\lambda)$ in ZrON/Si thin films prepared at different temperatures.

incomplete and that results in a comparatively low refractive index and specific $n(\lambda)$ function as it is shown in Fig. 3. At higher reaction temperatures, the $n(\lambda)$ functions are practically independent of technological conditions. It is interesting to point out that the refractive index of ZrON film is noticeably lower than that of ZrO_2 due to the presence of nitrogen [23]. Generally, the formation of interface SiO_2 layer with a detectable thickness was not found when oxide and oxynitride films were deposited on the Si substrate by different methods at a comparatively low temperature <500 °C [6,9,23–28]. The oxygen atoms needed for this reaction are captured from the oxide layer or provided by oxygen transport from the air by diffusion through the ZrO_2 layer [23,29,30].

4. Conclusions

The optical properties of ZrON/Si layer structures formed by oxidation/nitridation of metal Zr in the N_2O/Ar ambient are obtained with spectroscopic ellipsometry. Only incomplete oxidation is achieved at 500 °C and the refractive index of the films is comparatively low. The stabilization of high refractive index of ZrON films is achieved over the temperature range of 700–900 °C, but this is accompanied by SiO_2-based interface layer formation due to oxidation of the substrate material. This thermal effect is of great importance in the selection of technological conditions of complementary metal-oxide-semiconductor (CMOS) structures because the presence of SiO_2 interface layer generates the equivalent oxide thickness (EOT) value increase [31]. Thus, optimal electronic parameters of ZrON/Si structures should be found over the oxidation/nitridation temperature range of 500–600 °C.

Acknowledgments

The authors would like to acknowledge University of Malaya for providing the necessary facilities and resources for this research. This research was funded by the Ministry of Higher Education, Malaysia with the high impact research (HIR) grant number of UM.C/625/1/HIR/MOHE/ENG/27 and supported by the Academy of Sciences for the Developing World (TWAS) through TWAS-COMSTECH Research Grant.

Appendix A. Supporting information

Supplementary data associated with this article can be found in the online version at http://dx.doi.org/10.1016/j.matlet.2013.03.100.

References

[1] Wilk GD, Wallace RM, Anthony JM. Hafnium and zirconium silicates for advanced gate dielectrics. J Appl Phys 2000;87(1):484–92.
[2] Wallace RM, Wilk GD. High-*k* dielectric materials for microelectronics. Crit Rev Solid State Mater Sci 2003;28:231–85.
[3] Robertson J. Maximizing performance for higher *K* gate dielectrics. J Appl Phys 2008;104:124111.
[4] Lupina G, Schroeder T, Dabrowski J, Wenger Ch, Mane AU, Müssig H-J, et al. Praseodymium silicate films on Si(100) for gate dielectric applications: physical and electrical characterization. J Appl Phys 2006;99:114109.
[5] Pan T-M, Shu W-H. Structural and electrical characteristics of a high-*k* $NdTiO_3$ gate dielectric. Appl Phys Lett 2007;91:172904.
[6] Shvets VA, Aliev VSh, Gritsenko DV, Shaimeev SS, Fedosenko EV, Rykhlitski SV, et al. Electronic structure and charge transport properties of amorphous Ta_2O_5 films. J Non-Cryst Solids 2008;354:3025–33.
[7] Quah HJ, Lim WF, Wimbush SC, Lockman Z, Cheong KY. Electrical properties of pulsed laser deposited Y_2O_3 gate oxide on 4H-SiC. Electrochem Solid State Lett 2010;13(11):H396–8.
[8] Chin WC, Cheong KY. Effects of post-deposition annealing temperature and ambient on RF magnetron sputtered Sm_2O_3 gate on n-type silicon substrate. J Mater Sci—Mater Electron 2011;22(12):1816–26.
[9] Atuchin VV, Kalinkin AV, Kochubey VA, Kruchinin VN, Vemuri RS, Ramana CV. Spectroscopic ellipsometry and X-ray photoelectron spectroscopy of La_2O_3 thin films deposited by reactive magnetron sputtering. J Vac Sci Technol A 2011;29(2):021004.
[10] Li H, Lin L, Robertson J. Identifying a suitable passivation route for Ge interfaces. Appl Phys Lett 2012;101:052903.
[11] Cho HJ, Hwangbo CK. Optical inhomogeneity and microstructure of ZrO_2 thin films prepared by ion-assisted deposition. Appl Opt 1996;35(28):5545–52.
[12] Jiang X, Liu C, Lin F. Overview on the development of nanostructured thermal barrier coatings. J Mater Sci Technol 2007;23(4):449–56.
[13] Chevalier J, Gremillard L. The tetragonal-monoclinic transformation in zirconia: lessons learned and future trends. J Am Ceram Soc 2009;92(9):1901–20.
[14] Sato K, Abe H, Ohara S. Selective growth of monoclinic and tetragonal zirconia nanocrystals. J Am Chem Soc 2010;132:2538–9.
[15] Ling X, Li S, Zhou M, Liu X, Zhao Y, Shao J, et al. Annealing effect on the laser-induced damage resistance of ZrO_2 films in vacuum. Appl Phys 2009;48(29):5459–63.
[16] Wong YH, Cheong KY. Thermal oxidation and nitridation of sputtered Zr thin film on Si via N_2O gas. J Alloys Compd 2011;509:8728–37.
[17] Wong YH, Cheong KY. Metal-oxide-semiconductor characteristics of Zr-oxynitride thin film on 4H-SiC substrate. J Electrochem Soc 2012;159(3):H1–7.
[18] Wong YH, Cheong KY. Formation of Zr-oxynitride thin films on 4H–SiC substrate. Thin Solid Films 2012;520:6822–9.
[19] Rykhlitski SV, Spesivtsev EV, Shvets VA, Prokopiev VYu. Spectral ellipsometric complex ELLIPS-1771 SA. Instrum Exp Tech 2007;2:160–1 [in Russian].
[20] Ioffe Physical Technical Institute, RAS, Russia, *n*, *k* database of NSM, ⟨http://www.ioffe.rssi.ru/SVA/NSM/nk/⟩.
[21] Aspnes DE. The accurate determination of optical properties by ellipsometry. In: Handbook of optical constants of solids. Academic Press; 1985. p. 759–760.
[22] Wooten F. Optical Properties of Solids. New York: Academic Press; 1972.
[23] Ramana CV, Utsunomiya S, Ewing RC, Becker U, Atuchin VV, Aliev VSh, et al. Spectroscopic ellipsometry characterization of the optical properties and thermal stability of ZrO_2 films made by ion-beam assisted deposition. Appl Phys Lett 2008;92:011917.
[24] Atuchin VV, Kruchinin VN, Kalinkin AV, Aliev VSh, Rykhlitskii SV, Shvets VA, et al. Optical properties of $HfO_{2-x}N_x$ and $TiO_{2-x}N_x$ films prepared by ion beam sputtering. Opt Spectrose 2009;106(1):72–7.
[25] Ramana CV, Mudavakkat VH, Kamala Bharathi K, Atuchin VV, Pokrovsky LD, Kruchinin VN. Enhanced optical constants of nanocrystalline yttrium oxide thin films. Appl Phys Lett 2011;98:031905.

[26] Mudavakkat VH, Atuchin VV, Kruchinin VN, Kayani A, Ramana CV. Structure, morphology and optical properties of nanocrystalline yttrium oxide (Y_2O_3) thin films. Opt Mater 2012;34(5):893–900.
[27] Smith FW, Ghidini G. Reaction of oxygen with Si(111) and (100): critical conditions for the growth of SiO_2. J Electrochem Soc 1982;129(6):1300–6.
[28] Ma CY, Zhang QY. Interfacial layer growth of ZrO_2 films on silicon. Vacuum 2008;82(8):847–51.
[29] Larijani MM, Hasani E, Fathollahi V, Safa S. Thermally oxidized zirconium nanostructured films grown on Si substrates. Cryst Res Technol 2012;47 (4):443–8.
[30] Atuchin VV, Aliev VSh, Ayupov BM, Korolkov IV. Decreased refractive index of nanocrystalline zirconium oxide thin films. Int J Mod Phys B 2012;26(2):1250012.
[31] Robertson J. Interfaces and defects of high-*K* oxides on silicon. Solid-State Electron 2005;49:283–93.